Mekanika: Majalah Ilmiah Mekanika

Finite Element-Based Evaluation of Double-Hull Midsection Performance under Oblique Collision

Dina Malsyage¹, Aldias Bahatmaka^{1*}, Arnova Chandra Cahya Kirana¹, Lee Sang Won², Song Yeon Hee³

- 1 Department of Mechanical Engineering, Universitas Negeri Semarang, Semarang, Indonesia
- 2 Department of Fluid, Research and Development, Daewoo Shipbuilding and Marine Engineering, Geoje, South Korea
- 3 Department of Naval Architecture and Marine Systems Engineering, Pukyong National University, Busan, South Korea
- *Corresponding Author's email address: aldiasbahatmaka@mail.unnes.ac.id

Keywords:
Double-hull
Ship collision
Finite element analysis
Crashworthiness
ANSYS

Abstract

Ship collisions pose a significant concern in maritime safety, particularly for doublehull vessels operating in confined or high-risk areas. Understanding the structural response to collision is essential for improving crashworthiness. This study investigates the safety limits of a double-hull midsection ship under oblique impacts. Finite Element Analysis (FEA) was used to simulate three collision angles (45°, 60°, 90°) and four velocities (1, 3, 5, and 7 m/s). A benchmark study confirmed simulation accuracy with an error of less than 2%. The study reveals that impact angle and velocity significantly affect the ship's structural response. Perpendicular impacts (90°) with varying velocities produce the highest internal energy, reaching up to 28.99 MJ. In oblique impacts at 45°, the highest crushing force was generated, which reached 51.05 MN. Safety factor analysis indicates that impacts exceeding 3 m/s, especially those approaching perpendicular, lead to a decrease in structural integrity, falling below the acceptable limit. At 7 m/s and 90°, the stress on the inner hull exceeds the material's ultimate strength, indicating a potential for failure. To ensure structural safety, operational speeds should be limited to below 3 m/s. Findings highlight the importance of managing collision risks and guiding future ship design optimization.

1 Introduction

Maritime transport is crucial for global industrial growth, leading to more ships at sea and a higher risk of collisions. Although ship collisions are infrequent, their consequences can be severe, including structural damage, engine failures, human casualties, environmental pollution, hazardous materials, and economic losses from disruptions and repairs [1]. Improving the crashworthiness of ships is a key strategy to reduce the frequency and impact of these accidents [2]. A series of maritime collisions in recent months has underscored the critical importance of safety within the shipping industry. In April 2025, container ship KMTC Surabaya and bulk carrier Glengyle Hong Kong collided near Long Tau River, Vietnam, leading to an oil spill [3]. Concurrently, a tanker and a cargo ship collided off the coast of the United Arab Emirates, attributed to navigational misjudgment [4]. In May 2025, the Cuauhtémoc collided with the Brooklyn Bridge due to a systems failure [5].

https://dx.doi.org/10.20961/mekanika.v24i2.39924

Revised 11 August 2025; received in revised version 20 September 2025; Accepted 21 September 2025 Available Online 20 October 2025

2579-3144

121

Enhancing ship safety can be approached through two key strategies, namely active and passive safety [7]. Active safety focuses on technological advancements, including automatic navigation systems, anticollision radar, vessel traffic services, and comprehensive crew training. On the other hand, passive safety emphasizes the need to strengthen and assess the crashworthiness of ship structures, enabling them to absorb collision energy and prevent significant failures effectively. International Maritime Organization (IMO), through International Convention for the Safety of Life at Sea (SOLAS) Chapter II-1 requires the application of a double hull design on tankers and a probabilistic evaluation approach to collision incidents [8]. The Oil Pollution Act (OPA) 1990 requires all oil tankers operating in domestic waters to use a double hull structure to prevent spills [9]. Meanwhile, Det Norske Veritas-Germanischer Lloyd (DNV-GL) establishes technical guidelines for evaluating structural resistance to collisions through the Design against Accidental Loads procedure [10]. The Indonesian Classification Bureau (BKI) regulates similar provisions in its Rules for the Classification and Construction – Part 1: Seagoing Ships, Volume XVI, which lists the minimum dimensions for double bottoms and double sides on oil tankers according to the Common Structural Rules (CSR) standard [11]. Over the past decade, numerous studies have addressed the crashworthiness of ship structures, using both experimental and numerical approaches [12-15]. These include the Finite Element Method (FEM). [16] states that collisions involve essential factors, namely external dynamics and internal mechanics. The external dynamics refer to the overall movement of the ship during a collision, while the internal mechanics focus on the volume of damaged material.

In a previous study [17], a ship collision analysis was conducted at 25 points from the fore-end to the aft end. Simulations were performed at perpendicular collision angles, with speed variations ranging from 5 to 20 knots. As a result, the recommended speed in the strait area is only 5-10 knots in crossing situations. Additionally, the speed limit should be reduced to 5 knots when visibility and maneuverability are restricted. In this study, an expansion of the scenario was carried out at the midsection with various collision angles. The analysis is conducted to determine the behavior of damaged structures, such as buckling, folding, and tearing [18]. Therefore, this research aims to assess the structural suitability of a double-sided hull ship in various impact angles and speeds when subjected to a bulbous bow, particularly in confined water areas such as ports and straits, as well as during hazardous weather conditions. Additional calculations will be conducted by comparing simulation results with safety factors. Furthermore, structural behavior analysis will be performed to establish the operational safety limits of the ship in the event of potential collisions.

2 Numerical Methods

FEA is a numerical method used to evaluate a design's structural response to loads. FEM divides continuous objects into finite parts called elements [19], connected by nodes, allowing for the resolution of design problems through mathematical equations [20]. However, traditional solutions can be challenging for irregularly shaped objects. Thus, this study utilizes Rhinoceros 8 for geometric modeling, which is then exported to ANSYS 2020 for analysis and simulation. The process comprises three stages: pre-processing, where the model geometry, material properties, boundary conditions, and mesh are defined; solving, which calculates the system's response; and post-processing, where simulation results are interpreted for further analysis.

2.1 Theoretical background

Two critical parameters for evaluating structural resistance in crashworthiness assessments related to ship collisions are absorbed energy and crushing force. In ship collisions, absorbed energy denotes the energy dissipated through the plastic deformation or damage sustained by the ship's structure during impact [21]. This parameter reflects the energy necessary to induce permanent deformation or rupture in various hull components. Conversely, crushing force refers to the magnitude of force experienced by the ship's structure at the contact point when it is penetrated by the colliding vessel. This force is not constant; instead, it fluctuates as the material yields and ultimately reaches the point of failure. Previous research proposed an empirical approach (see Equation 1) [16].

$$E = 47.2R + 32.7 \tag{1}$$

This formula connects the absorbed energy E (measured in megajoules, MJ) to the volume of crushed material R (measured in cubic meters, m^3) and is commonly used in the analysis of ship accidents. After that, [23-24] formulated two empirical analyses between absorbed energy and the volume of material damage from two absorbed energy mechanisms (plastic tension deformation and crushing damage), with two empirical formulas (see Equations 2 and 3).

$$E_1 = 0.77 \times \varepsilon_f \times \sigma_0 \times R_1 \tag{2}$$

$$E_2 = 3.5 \times \frac{t}{b} \times 0.67 \times \sigma_0 \times R_2 \tag{3}$$

The first energy absorption mechanism, plastic tension deformation (represented by E_1), occurs during the indentation of the shell plating in side collisions, where the material undergoes tensile stretching until it ruptures. The second mechanism, folding and crushing damage (represented by E_2), involves large plastic deformations, such as the crushing of the bow or the crushing and folding of the deck structure, which dissipate energy through progressive plate buckling. Accordingly, ε_f is the failure strain, σ_0 is the flow stress, R_1 is the volume of tension-damaged structural members, t is the plate thickness, t is the width of the damaged plate, and t is the volume of crushed structural members.

2.2 Benchmark study

A benchmark study is used to ensure the reliability and accuracy of the simulation by comparing results with previous data through force-displacement analysis [17-25]. It involves a quasi-static penetration test using a conical indenter to penetrate the hull structure. Quasi-static analysis effectively captures the essential structural response under low-velocity impact (see results in Figure 1).

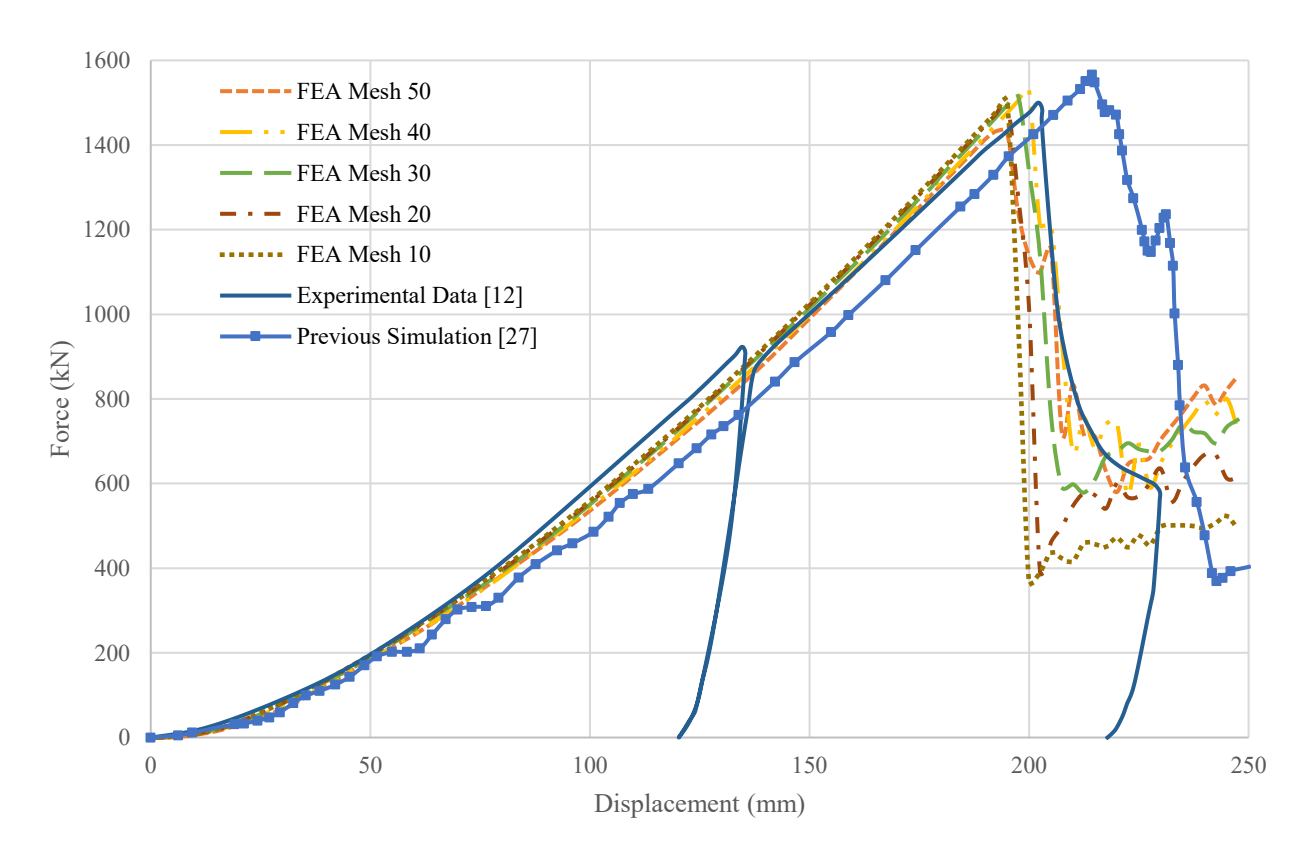


Figure 1. Comparison of the force-displacement curve in this study with previous research

This validation is founded on previous studies conducted at a 1:3 scale typical for medium-sized tankers [12]. The plate measures 720 mm x 1200 mm x 5 mm and is constructed from mild steel (S235JR, EN 10025). Meanwhile, the conical indenter features a nose radius of 200 mm with a 90° spreading angle. The material used is structural steel. The simulation was performed using the ANSYS Workbench 2020 R2 interface, with the LS-DYNA solver employed for the nonlinear finite element analysis. The indenter's penetration is simulated with a controlled velocity of 1.67 m/s, accelerated to 1000 times the experimental speed while maintaining a quasi-static condition, as significant inertia effects are negligible below 10 m/s [25]. The indenter is considered rigid and restricted to movement along the impact direction, while the plate is firmly fixed at all four edges. All components are modeled as shell elements using the Belytschko-Lin-Tsay formulation with five integration points. Previous studies suggest an Element Length-to-Thickness (ELT) ratio of 5-10 [26]. For this validation, ELT ratios ranging from 2 to 10 were applied to determine an appropriate mesh size.

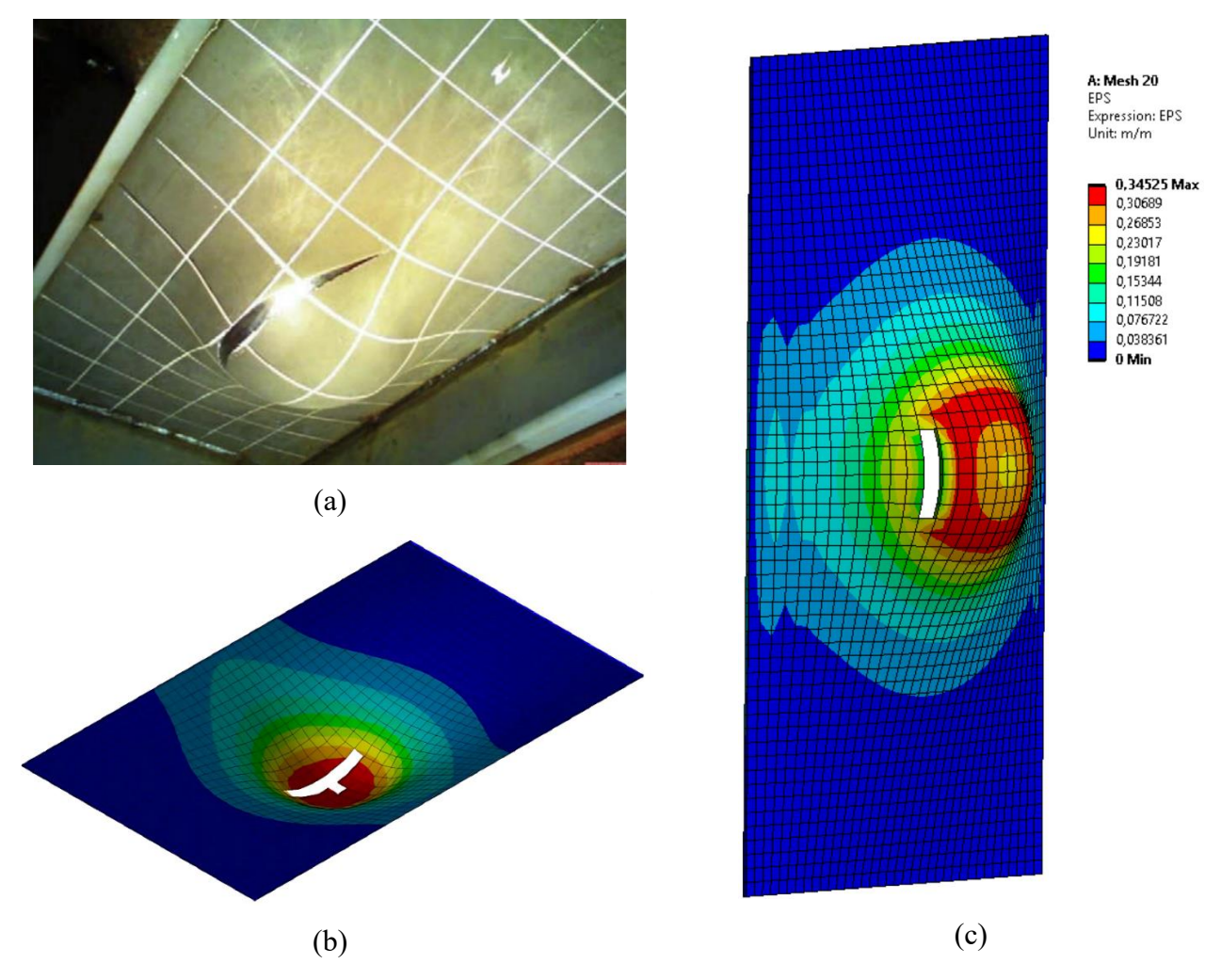


Figure 2. Comparison of simulation results: (a) Laboratory experiment by [12], (b) Pioneer finite element simulation by [27], and (c) Simulation results in this study with the mesh size of 20 mm

The comparison of the force-displacement curves is illustrated in Figure 1. Previous research [27] (see Figure 2b) recorded a maximum crushing force of 1560 kN at a displacement of 215 mm. In contrast, the experimental results [12] (refer to Figure 2a) showed a maximum crushing force of 1500 kN at a displacement of 200 mm. The current study (Figure 2c) demonstrates that simulations using mesh sizes of 10, 20, and 30 mm provide a more accurate replication of experimental results, including maximum forces of 1506 kN, 1501 kN, and 1516 kN, respectively, and fracture displacement at 195 mm, 195 mm, and 197.5 mm, respectively. Meanwhile, simulations using a coarser mesh size (40 and 50 mm) yield maximum forces of 1530 kN and 1433 kN at displacements of 202.5 mm and 192.5 mm, respectively.

Overall, the error in the finer mesh size of 10-30 mm is less than 2% compared to the experimental and previous simulation. Meanwhile, there is around 4% error in the coarser mesh. The selection of mesh size based on the Element Length-to-Thickness ratio (4-6) closely resembles the comparative data, while maintaining time and cost efficiency. In conclusion, both the data from previous studies and current simulations show strong agreement and correlation.

2.3 Material assignment

The material selected for the struck and the striking model in this study is mild steel (S235JR EN10025) and structural steel according to [27] with mechanical properties derived from previous research [12]. The struck model material is assumed to exhibit isotropic plastic behavior, and the true stress-strain relationship of the material in the plastic region is modeled using a Power-Law expression [13], defined as:

$$\sigma = K \cdot \varepsilon^n \tag{4}$$

where σ is the true stress, ε is the true plastic strain, K is the strength coefficient, and n is the strain hardening exponent. Meanwhile, the striking model used structural steel, as shown in Table 1.

 Table 1. Mechanical properties of the materials

Material	$\rho (kg/m^3)$	E (GPa)	v	σ _y (MPa)	σ _{UTS} (MPa)	K (MPa)	n	Ef
S235JR EN10025	7800	210	0.3	285	416	740	0.24	0.35
structural steel	7850	200	0.3	250	460	-	-	-

2.4 Modeled design

The structural design of ships transporting dangerous goods or passengers must comply with the Oil Pollution Act (OPA) of 1990 and relevant International Maritime Organization (IMO) regulations. This is in accordance with Biro Klasifikasi Indonesia's Rules for the Classification and Construction, specifically Part 1: Seagoing Ships, Volume XVI-IACS Common Structural Rules for Double Hull Oil Tankers (2014 Edition), particularly Section 5, No. 3. Compliance includes adhering to minimum structural dimensions, such as:

The minimum double bottom depth, d_{db} , is to be taken as the lesser of, as stated in Equation 5, but not less than 1.0 m.

$$d_{db} = \frac{B}{15} \,\mathrm{m} \tag{5}$$

Where, B is moulded breadth, in m, defined as the maximum breadth of the ship, measured amidships to the moulded line of the frame (Section 4/1.1.3.1).

The minimum double-sided width, w_{ds} , is to be taken as the lesser of, as stated in Equation 7, but not less than 1.0 m.

$$w_{ds} = 0.5 + \frac{DWT}{20000} \,\mathrm{m} \tag{6}$$

Where, DWT is the deadweight of the ship, in tonnes, floating in water with a specific gravity of 1.025, at the summer load line draught (Section 4/1.1.14.1).

The scenario features an oil tanker ship as the struck ship (Figure 3a), with the following dimensions: Length L=140 m, Breadth B=22 m, Depth H=9 m, and DWT=10,000 t. The striking ship (Figure 3b) is a bulbous bow from a 134 m container ship. The struck ship only takes half of the total height of the side hull (lower section) to determine its behavior in collision with the bulbous bow. In this study, the struck ship is modeled as a thin-walled, deformable structure with a uniform thickness of 15 mm, allowing for effective capture of its structural responses. The material used for this ship is S235JR EN10025. In contrast, the striking ship is treated as a rigid structure made from structural steel.



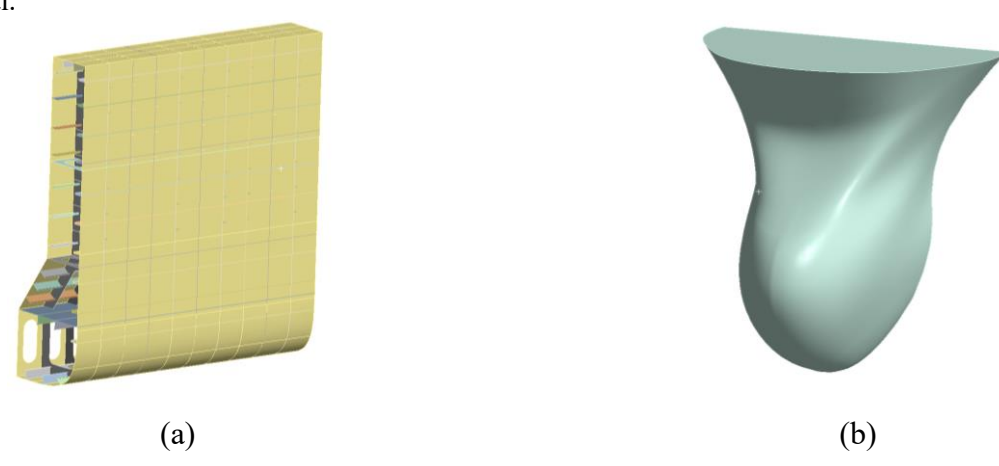


Figure 3. Modeled design for collision analysis in this study: (a) The struck ship (lower section of double hull) and (b) The striking ship (bulbous bow)

2.5 Configuration for finite element simulation

The modeled design utilized a 75 mm mesh size, employing four-node shell elements that incorporate five integration points throughout their thickness. This is also known as the Belytschko-Lin-Tsay shell element formulation, as referenced in [28]. When the plastic strain reaches the specified value of effective plastic strain indicative of failure, the element is removed from the analysis. A friction coefficient of 0.3 is applied, as mentioned in [29-31].

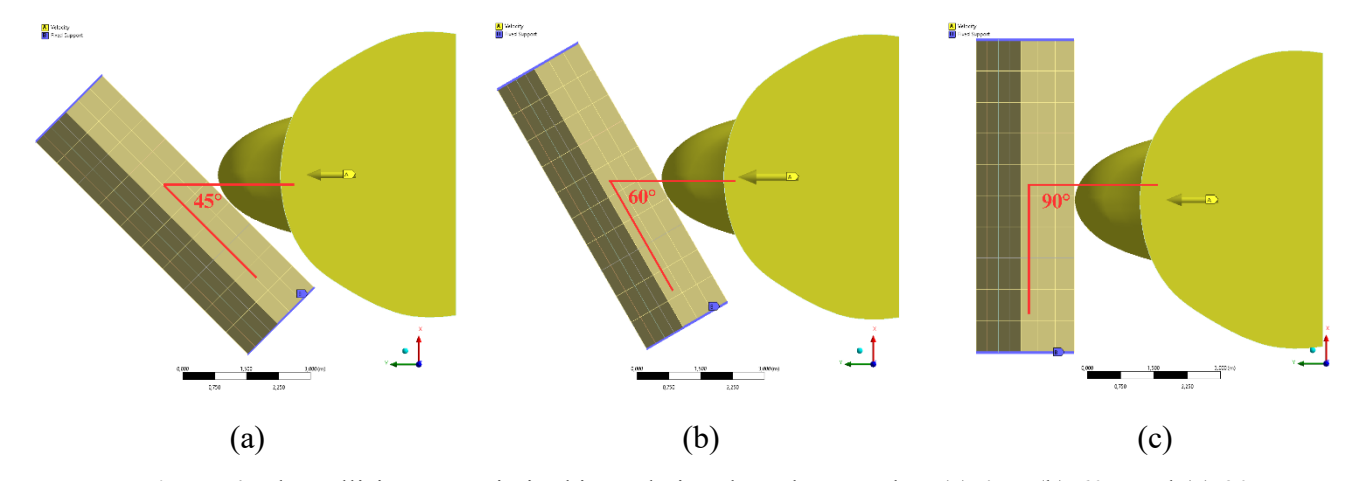


Figure 4. The collision scenario in this study involves three angles: (a) 45°, (b) 60°, and (c) 90°

As seen in Figure 4, three collision angles were proposed in this study: 45°, 60°, and 90°. Each is paired with velocity variations of 1 m/s, 3 m/s, 5 m/s, and 7 m/s, which is considered reasonable for ship operations leading up to a potential collision [32]. This parameter is used to analyze the behavior of the double-hull side structure during impact. Fixed supports are installed on all side edges of the struck ship, and the striking ship is only permitted to move translationally in the collision direction (Uy direction, see Figure 4). Additionally, all rotational movements are inhibited, and a termination time of 0.203 seconds is set. These configurations are selected to represent a worst-case scenario, allowing for the evaluation of the side structure's ultimate strength under impact loading, with particular attention to the post-collision condition of the inner shell [33]. The mass scaling is added in this study at a rate of less than 3.5%. The mass scaling technique enables the addition of nonphysical mass to a structural analysis, facilitating larger explicit time steps and significantly reducing computational costs. This approach is prevalent in many Finite Element Analysis (FEA) software packages. Within the LS-DYNA solver, mass scaling is applied by adjusting the specified time-step size. As a result [34], similar outputs were achieved for the force-displacement and absorbed energy graphs, along with a reduction in computational time of up to 40% for quasi-static simulations.

3 Results and Discussion

When analyzing the effects of side impacts on the structure of double hull ships, evaluating crashworthiness and failure tendencies depends on the energy absorbed by the structure during the impact. This energy, represented by the internal energy value at the end of the simulation, indicates the accumulated strain energy due to plastic deformation during the contact between the striker and the structure. The higher the energy absorbed, the better the structure can endure the impact without experiencing catastrophic failure. This study analyzes not only physical energies, such as internal energy and crushing force, but also the numerical aspects of impact simulation by evaluating hourglass energy values. Zero-energy modes, also known as hourglass energy, occur in FE models that use under-integrated element formulations. Such modes produce artificial zero-strain and zero-stress conditions, which ultimately give rise to inaccurate force—time responses and pronounced element distortion [35].

Hourglass energy is generated from the finite element of non-physical numerical energy and can serve as an indicator of the simulation's stability and accuracy. According to ANSYS Guidelines [20], hourglass energy acts as a control parameter for assessing the quality of the numerical solution. From the simulation results (Table 2), it is indicated that while hourglass energy increases with higher impact velocities, its loss remains significantly below the internal energy [26]. At the end of the impact process, the contribution of hourglass energy to the total internal energy is less than 1.1%. This figure suggests that the numerical error in the simulation is within acceptable limits [36]. Hence, the simulation model is reliable and accurate in describing the ship's structural response during the impact event.

Section	Angle (°)	Speed (m/s)	Internal Energy (MJ)	Hourglass Energy (MJ)	Crushing Force (MN)
	45	1	0.96	0.006	12.44
		3	7.34	0.069	25.73
		5	16.67	0.168	39.39
		7	27.67	0.280	51.05
	60	1	1.41	0.008	15.57
		3	7.34	0.069	25.73
midsection		5	17.36	0.191	29.27
		7	25.50	0.290	32.79
	90	1	1.69	0.011	15.80
		3	10.33	0.088	29.74
		5	20.27	0.178	34.35
		7	28.99	0.290	34.29

Table 2. Simulation results based on the collision angle and speed

3.1 Influence of impact angle and velocity

Figure 4 illustrates the relationship between angle and velocity in the structural response of the modeled collision. The data presented corresponds to three impact angle variations: 45°, 60°, and 90°. In Fig. 5a, an impact angle of 90° produces the highest energy at all speed levels, indicating that perpendicular (normal) impacts cause the most significant deformation and maximum energy absorption. This is because the force direction is completely perpendicular to the plane of the structure, resulting in high energy transfer. Conversely, a 60° angle produces the lowest internal energy, as some of the impact energy is not directed directly to the surface but is instead dissipated as shear or sliding energy. A 45° angle is in the middle. Still, it shows a significant increase in internal energy, which is the additional resistance of the double hull structures, such as frames and stiffeners, to impact and damage as they deform at higher speeds and reach the inner hull. A similar trend is observed in the crushing force graph (Figure 5). The 45° angle produces the highest crushing force, especially at a speed of 7 m/s. This indicates that in oblique collisions, the impact force is more distributed throughout the structural components and causes local deformation [37]. A 60° collision angle results in lower forces at all speeds, suggesting less efficient interaction between the bulbous bow and hull, particularly at higher speeds.

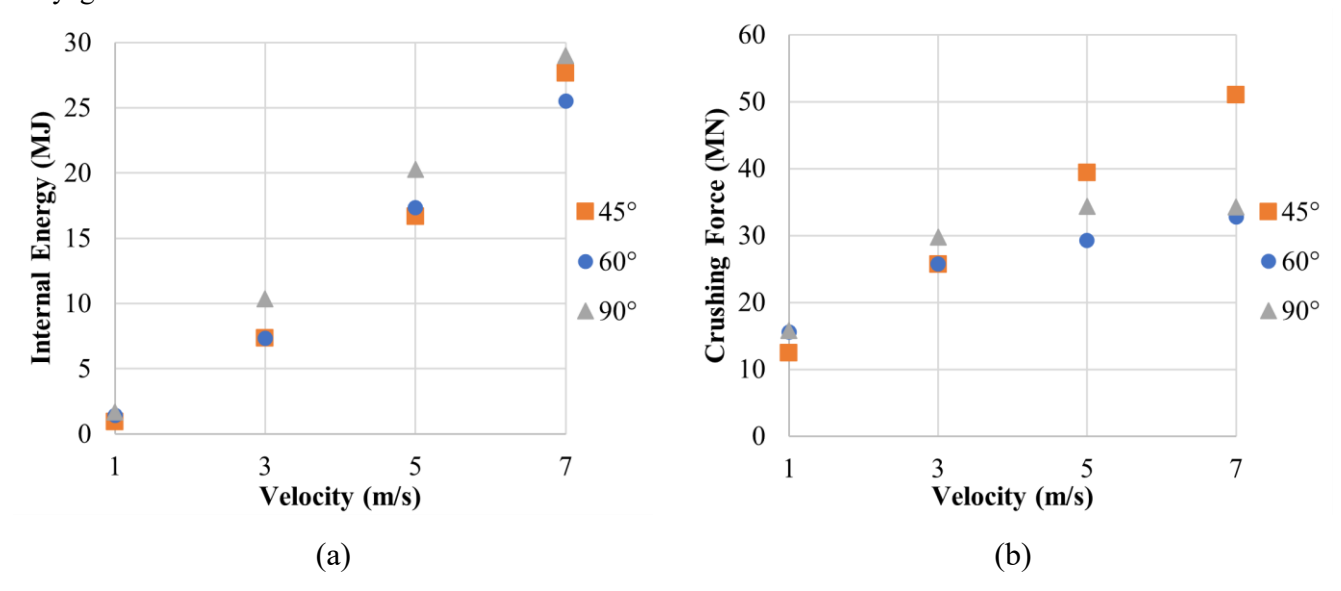


Figure 5. Structural characteristics of the double hull response to the modeled collision: (a) Internal energy and (b)

Crushing force

This leads to reduced resistance to impact and potential for severe damage. At a 90° angle and a speed of 7 m/s, the crushing force significantly decreases compared to a 45° angle, indicating weaker inner hull resistance. In contrast, collision angles between 0° and 45° enable the ship's structure to withstand impacts more effectively, as double-hull components, such as stiffeners and frames, absorb damage. As a result, the structure experiences both shear and sliding, which helps prevent the fatal failure of the inner hull [38]. Conversely, if the collision angle approaches 90°, the structure's resistance to impact loads tends to decrease, indicating structural failure that results in more intensive damage to the inner hull. In addition, in the case of an oblique collision, the displacement required is more protracted to reach the inner hull than in the perpendicular case. Therefore, it is necessary to pay attention to how the structural response works, considering the basic behavior of the ship structure. This is because the midsection tends to experience bending loads during its operation due to phenomena such as hogging and sagging [39].

Based on Figures 6 and 7, the impact velocity significantly influences the response of the ship's structure, both in terms of the internal energy absorbed and the resulting crushing force. At the lowest speed rate of 1 m/s, the internal energy absorbed by the structure is minimal, ranging from 1 to 2 MJ (see Table 2) for all impact angles. The crushing force is also relatively low, at around 12-16 MN, indicating that the structure has not undergone significant deformation at this speed (see Figures 8a, 9a, and 10a). However, when the velocity reaches 3 m/s, both the internal energy and the impact force increase sharply, especially for the 90° angle, which yields values of around 10 MJ for internal energy and over 30 MN for the crushing force. The structure started to experience significant deformation (Figure 10b). At a speed of 5 m/s, the spike in energy and force becomes more pronounced. The internal energy absorbed reaches approximately 16-20 MJ, depending on the impact angle, and the crushing force increases to 39.39 MN, particularly at a 45° angle. This indicates that the structure has suffered more serious damage and is beginning to lose its elastic impact-resistance capacity, particularly in the outer hull (see Figures 8c, 9c, and 10c). However, as seen in Figure 7, at speeds of 1-5 m/s, the crushing force fluctuation remains stable, indicating that the striker continues to penetrate the outer hull. When the speed approached 7 m/s, both the internal energy and impact force reached maximum values. At a 90° angle, the highest internal energy of 28.99 MJ is observed, while a 45° angle produces the highest crushing force, reaching 51.05 MN. This indicates that at high speeds, the outer hull structure undergoes plastic deformation, and its energy absorption capacity increases dramatically, depending on the impact angle. As seen in Figure 7, significant fluctuations in the crushing force and the end of the impact time indicate that the striker has reached the inner hull side (see Figures 8, 9, and 10). Therefore, the higher the impact speed, the greater the potential damage to the ship's structure, both in terms of absorbed energy and the resulting reaction forces.

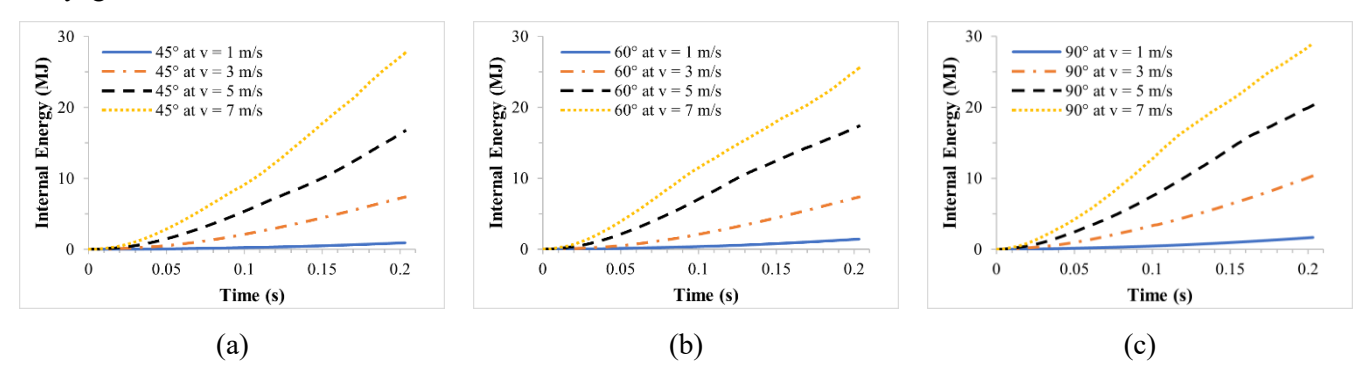


Figure 6. Increase in internal energy in the modeled scenario, considering the striking speed:

(a) 45° , (b) 60° , and (c) 90°

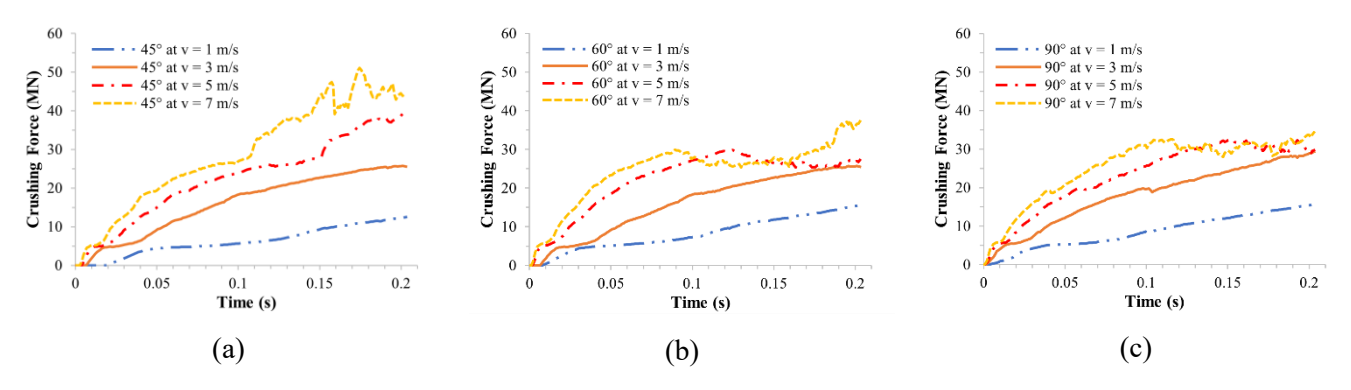


Figure 7. Fluctuations in crushing force in the modeled scenario considering the striking speed:

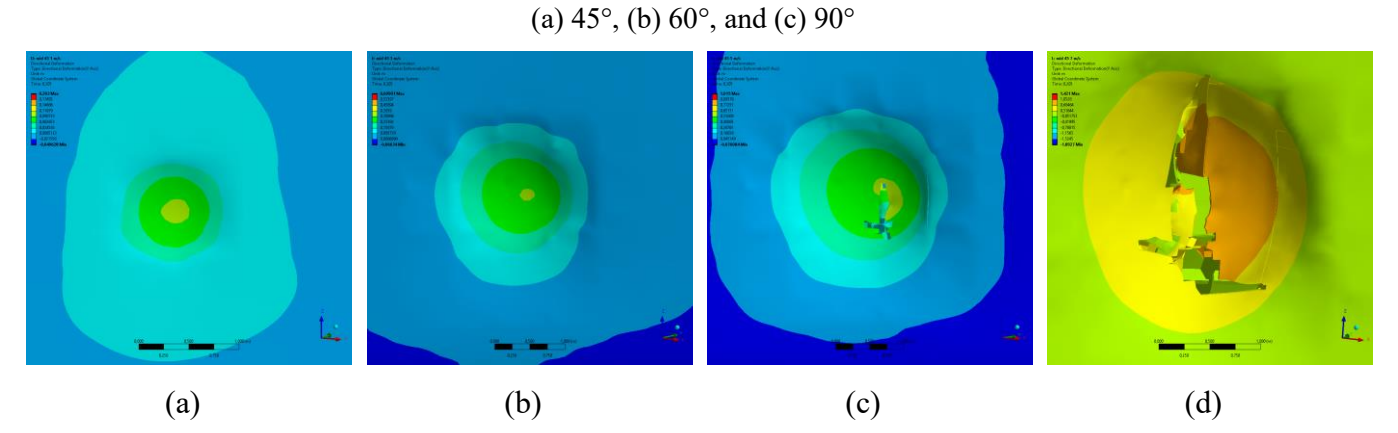


Figure 8. Deformation contour of the collision angle 45° at speed: (a) 1 m/s, (b) 3 m/s, (c) 5 m/s, and (d) 7 m/s

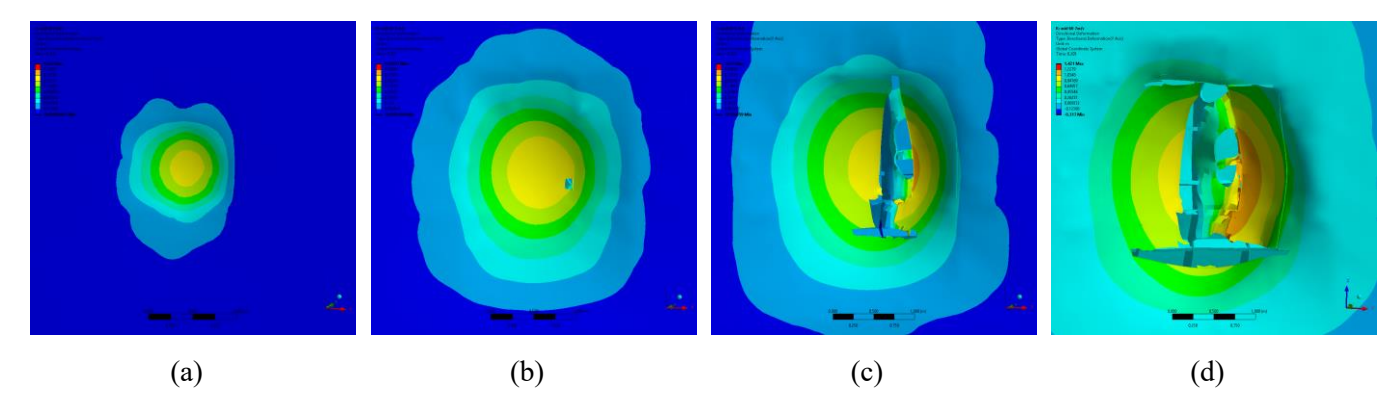


Figure 9. Deformation contour of the collision angle 60° at speed: (a) 1 m/s, (b) 3 m/s, (c) 5 m/s, and (d) 7 m/s

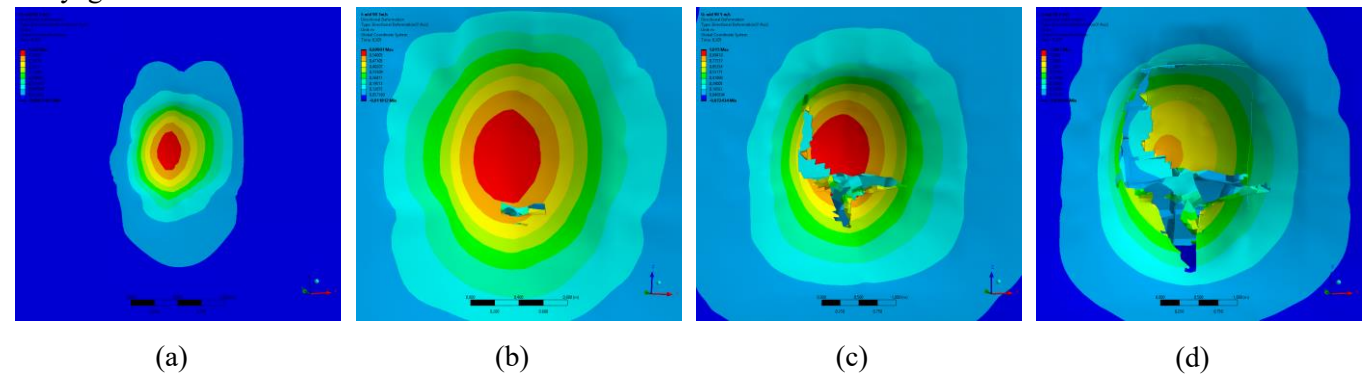


Figure 10. Deformation contour of the collision angle 90° at speed: (a) 1 m/s; (b) 3 m/s; (c) 5 m/s, and (d) 7 m/s

3.2 Safety factor of speed limit

Navigation safety is crucial in the maritime industry, requiring adherence to international regulations such as the International Regulations for Preventing Collisions at Sea (COLREGs), established by the International Maritime Organization (IMO). These regulations provide rules to prevent collisions between vessels on both open seas and in confined waters. Rule 6 of the COLREGs focuses on Safe Speed, stating that vessels must operate at a speed that allows for proper avoidance of collisions and stop within a suitable distance for the conditions. Although it does not establish a specific speed limit, it requires the crew to consider factors such as visibility, maritime traffic, vessel maneuverability, and weather when determining a safe speed.

Low speeds are typically used when ships enter or exit ports, navigate narrow or shallow waters, or operate in areas with heavy maritime traffic. Additionally, maintaining low speeds is crucial during adverse weather conditions or limited visibility, such as dense fog or heavy rain, as it allows the crew to respond more effectively. This practice is also crucial during dock approaches and boarding procedures to ensure the ship's precise and stable movements. Moreover, low speeds are necessary to comply with Emission Control Areas / Sulphur Emission Control Areas (ECAs/SECAs) and when navigating through regions prone to ice or floating debris, which helps minimize the risk of hull damage. Consequently, reducing speed in these situations is a vital component of risk management in ship operations, aiming to uphold safety, efficiency, and maritime security.

Based on the analysis results obtained in the previous subsection, a comparison was made between the internal energy generated by impact loads and the safety estimate, represented by the Safety Factor (SF). In this study, the safety factor is defined as the ratio between the yield state and the working state. The yield condition refers to the structural failure at an impact speed of 7 m/s. In contrast, the working conditions were analyzed across three speed scenarios: 1 m/s, 3 m/s, and 5 m/s, to determine the SF value for each scenario. The main parameter used in this evaluation is internal energy, which indicates the amount of energy absorbed by the double-sided hull structure due to impact, as mentioned in [17]. The internal energy values are derived from the data presented in Table 2, while the calculation of the SF values is shown in Table 3.

This evaluation was conducted at impact angles of 45°, 60°, and 90° to determine how well the structure absorbs impact energy before reaching the failure condition. The results of this comparison are also used to assess whether the structure meets the safety criteria recommended in the literature [40]; a similar method was utilized in [17]. According to the safety factor calculations in Table 3, all structural components subjected to an impact velocity of 1 m/s remain within a high margin of safety. At this velocity, all impact angles yield safety factor values that exceed the recommended limits for all types of loads, including static, repeated, variable, change, fatigue, and impact loads. However, at a velocity of 3 m/s, the safety factor values only met safety standards for short-term and long-term static loads, but are unacceptable for repeated, variable change, fatigue, and impact loads.

Table 3. Safety factor calculation considering internal energy

Angle Calculated Factor				Load Type [40]					
(°)	(°) 1 m/s 3 1	3 m/s	5 m/s	Static Short-Term	Static Long-Term	Repeated	Variable Change	Fatigue	Impact
45	28.88	3.77	1.66						
60	18.15	3.47	1.47	1-2.5	2.0-5	5.0-15	4.0-10	5.0-10	10.0-15
90	17.20	2.81	1.43						

This condition worsens significantly at a speed of 5 m/s, where the safety factor values drop below the minimum threshold for only short-term static loads, indicating a high risk of structural failure under real-world impact conditions. In addition to velocity, the impact angle also affects the amount of energy the structure must absorb; larger impact angles (closer to perpendicular, 90°) tend to increase absorbed energy and decrease the safety factor values. Therefore, collisions at speeds above 3 m/s, particularly at 90° angles, pose serious structural risks because the safety factor is below the recommended limit for most load types. The structural integrity of a vessel's inner hull is critical during collisions or impacts, especially in marine environments where various speeds and angles of impact can occur. Figure 11 shows the stress contour on the inner hull. To ensure safety and durability, it is crucial to assess whether the hull can withstand the stresses generated under these conditions.

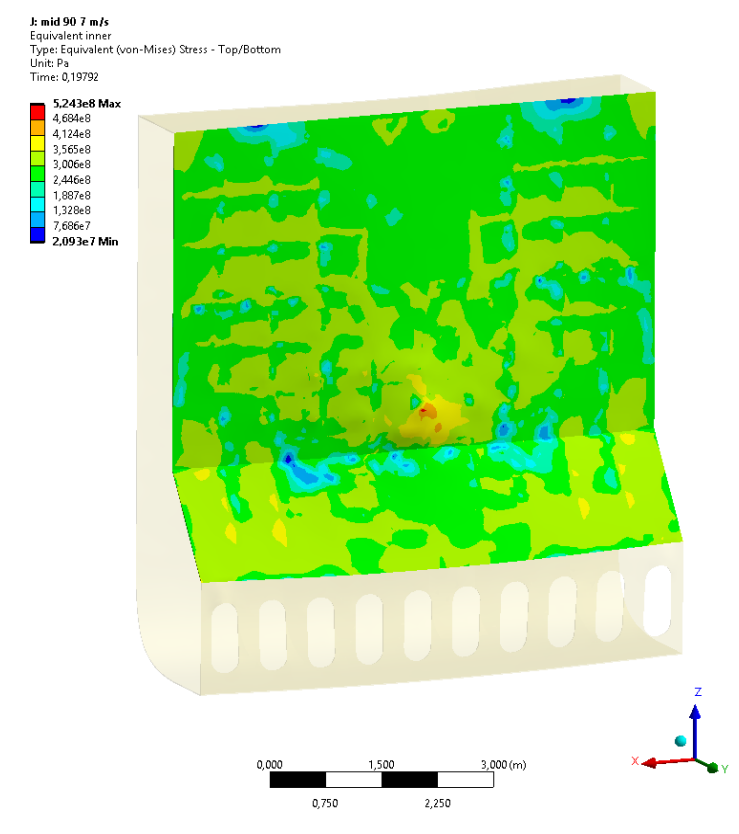


Figure 11. Stress distribution along the inner hull at 90° impact angle during 7 m/s collision

Table 4 presents a detailed evaluation of the stress response of the inner hull midsection under various collision angles (45°, 60°, and 90°) and velocities ranging from 1 m/s to 7 m/s. The maximum stress values obtained from each scenario are compared to the ultimate stress limit of 416 MPa, as defined in the BKI Rules Vol. V, 2025, Section 4B, 6.2. From this comparison, a safety factor is derived by dividing the ultimate stress by the maximum stress experienced in each case [41]. A safety factor greater than 1.1 is considered acceptable for structural performance under impact loading [41]. The results show that for all collision angles, impact speeds between 1 m/s and 5 m/s produce safety factors greater than 1.1. This indicates that the inner hull can withstand side collisions within this speed range without exceeding the material's structural limits.

However, as the collision speed increases to 7 m/s, the safety factor decreases significantly, especially at higher impact angles. As seen in Figure 11, a 90° collision at a speed of 5 m/s yields a safety factor of only 1.07. At 7 m/s, the maximum stress reaches 524.29 MPa, resulting in a reduction of the safety factor to 0.79. This value indicates a high risk of structural failure due to stress exceeding the material's capacity, particularly in perpendicular impacts where energy transfer is most severe.

Table 4. Stress status for inner hull

Section	Angle (°)	Speed (m/s)	Maximum Stress (MPa)	Ultimate Stress Material (MPa)	Safety Factor	Stress Status
midsection inner hull	45	1	289.60	416	1.44	accepted
		3	360.00	416	1.16	accepted
		5	374.18	416	1.11	accepted
		7	407.99	416	1.02	not accepted
	60	1	295.66	416	1.41	accepted
		3	354.65	416	1.17	accepted
		5	363.90	416	1.14	accepted
		7	411.25	416	1.01	not accepted
	90	1	301.59	416	1.38	accepted
		3	351.59	416	1.18	accepted
		5	389.98	416	1.07	not accepted
		7	524.29	416	0.79	not accepted

To ensure structural integrity and safety, operational speeds should be limited to conditions that maintain a safety factor above the minimum threshold, particularly with regard to impact and fatigue loads. However, it's essential to recognize that while the safety factor offers a quantitative assessment of a structure's capacity, the risk of collision doesn't rely solely on structural strength. Human factors, such as crew decision-making and errors, along with environmental conditions like weather, visibility, vessel maneuverability, and operational practices, significantly influence the prevention of collisions and the mitigation of their consequences. Therefore, maintaining a high safety factor at low speeds must be complemented by strong operational measures to guarantee overall safety.

4 Conclusions

The results indicate that a structure's ability to absorb energy and resist failure is significantly influenced by both the angle and velocity of impact. In particular, higher speeds and perpendicular impacts result in greater damage, with the most severe damage occurring at a 90 ° angle. Quantitative data reveal that at impact speeds of 7 m/s, the internal energy increases by approximately 90% compared to impacts at 1 m/s. The maximum internal energy recorded during simulations was around 28.99 MN for 90° impacts at 7 m/s, approximately 27.67 MN at 45°, and 25.5 MN at 60°, all under the same speed conditions. The capacity to resist crushing forces decreases as the angle of collision approaches a perpendicular angle. The results indicate that at an angle of 45°, the crushing force is 51.05 MN, which decreases by 32% to 34.39 MN at a 90° angle, thereby reducing the structural safety margin. Hourglass energy remained within acceptable limits across all scenarios, confirming the reliability of the numerical model. The findings suggest that impact speeds exceeding 3 m/s, particularly at high impact angles, pose significant risks to structural integrity, with safety factors dropping below the recommended level of 1.5 in some instances. Based on these results, it is proposed that operational safety limits should keep impact speeds below 3 m/s when navigating confined waters or hazardous conditions to prevent critical damage. These insights inform design improvements for ship crashworthiness, emphasizing the importance of managing impact angle and velocity to enhance maritime safety. Future research is recommended to focus on refining ship structural designs by exploring diverse geometric configurations and advanced material alternatives. Expanding the analysis to encompass a broader range of collision scenarios, such as fluid-structure interaction, multi-body interactions, and varied material properties, may provide a more comprehensive understanding of structural performance. The application of optimization techniques and probabilistic approaches is also suggested to improve crashworthiness and enhance safety margins under realistic operating conditions.

5 Acknowledgement

The author would like to express sincere gratitude to the Department of Mechanical Engineering at Universitas Negeri Semarang for the valuable support provided. This support has been instrumental from the Faculty of Engineering under Contract Number: 139.03.2.693449/2025.05/2025, Universitas Negeri Semarang.

References

- 1. R. A. Rahman, S. Suryanto, A. R. Prabowo, I. Yaningsih, S. Ehlers, and M. Braun, "Assessment of ship collision risk based on the recorded accident cases: Structural damage and environmental recovery," *E3S Web Conf.*, vol. 563, pp. 1-8, 2024.
- 2. Z. Wang, Z. Hu, K. Liu, and G. Chen, "Application of a material model based on the Johnson-Cook and Gurson-Tvergaard-Needleman model in ship collision and grounding simulations," *Ocean Eng.*, vol. 205, article no. 106768, 2020.
- 3. R. Raza, *Ship Collision Causes Oil Spill on Vietnam's Long Tau River*, Marine Traffic. Available in https://www.marinetraffic.com/en/maritime-news/14/accidents/2025/12041/ship-collision-causes-oil-spill-on-vietnams-long-tau-river. (Accessed in July 10, 2025).
- 4. J. Gross and N. Ismaeel, *Oil Tanker Collision Near Strait of Hormuz Raises Security Fears*, The New York times. Available in https://www.nytimes.com/2025/06/19/business/tanker-collision-hormuz-israel-iran.html. (Accessed in July 15, 2025).
- 5. K. Sheehan, B. Kathianne, A. Blair, and J. F. Gibbon, *Mexican ship crashed into Brooklyn Bridge because it lost steering during mechanical failure*: sources, New York Post. Available in https://nypost.com/2025/05/18/us-news/mexican-ship-crashed-into-bklyn-bridge-because-it-lost-steering-during-mechanical-failure-sources/. (Accessed in July 15, 2025).
- 6. G. Wright, *North Sea tanker collision what we know so far*, BBC News. Available in https://www.bbc.com/news/articles/c62z9ee68y6o. (Accessed in July 15, 2025).
- 7. W. Ma, Y. Zhu, M. Grifoll, G. Liu, and P. Zheng, "Evaluation of the Effectiveness of Active and Passive Safety Measures in Preventing Ship-Bridge Collision," *Sensors.*, vol. 22, no. 8, article no. 2857, 2022.
- 8. International Maritime Organization, *International Convention for the Safety of Life at Sea (SOLAS)*Chapter II-1 Construction Structure, subdivision and stability, machinery and electrical installations. International Maritime Organization, London, 1974.
- 9. K. W. Ketkar, "The Oil Pollution Act of 1990: A Decade Later," *Spill Sci. Technol. Bull.*, vol. 7, no. 1-2, pp. 45-52, 2002.
- 10. Det Norske Veritas, "Design Against Accidental Loads," *Recomm. Pract. DNV-RP-C204*, no. October, pp. 7-52, 2010.
- 11. Biro Klasifikasi Indonesia, "IACS Common Structural Rules For Double Hull Oil Tankers," *Rules Classif. Constr. Part 1. Seagoing Ships*, vol. XVI, 2014.
- 12. H. S. Alsos and J. Amdahl, "On the resistance to penetration of stiffened plates, Part I Experiments," *Int. J. Impact Eng.*, vol. 36, no. 6, pp. 799-807, 2009.
- 13. P. Hogström and J. W. Ringsberg, "An extensive study of a ship's survivability after collision A parameter study of material characteristics, non-linear FEA and damage stability analyses," *Mar. Struct.*, vol. 27, no. 1, pp. 1-28, 2012.
- 14. A. Jahanbakhsh, J. Fragasso, L. Moro, and M. M. S. Islam, "Finite Element Model Updating of a Scale Model Ship Using Experimental Modal Analysis and Response Surface Methodology," *J. Mar. Sci. Appl.*, pp. 1-17, 2025.
- 15. X. Liu, H. Wu, and D. Chen, "Impact force-damage depth model for ship-bridge collision," *Eng. Fail. Anal.*, vol. 167, article no. 108963, 2025.
- 16. V. U. Minorsky, "An analysis of ship collisions with reference to protection of nuclear power plants," *J. Ship Res.*, vol. 3, pp. 1-4, 1958.

- 17. A. R. Prabowo, D. M. Bae, J. H. Cho, and J. M. Sohn, "Analysis of structural crashworthiness and estimating safety limit accounting for ship collisions on strait territory," *Lat. Am. J. Solids Struct.*, vol. 14, no. 8, pp. 1594-1613, 2017.
- 18. B. C. Cerik and J. Choung, "Fracture Estimation in Ship Collision Analysis-Strain Rate and Thermal Softening Effects," *Met.*, vol. 11, no. 9, article no. 1402, 2021.
- 19. A. R. Prabowo, A. Bahatmaka, J. H. Cho, J. M. Sohn, D. M. Bae, S. Samuel, and B. Cao, "Analysis of structural crashworthiness on a non-ice class tanker during stranding accounting for the sailing routes," *Marit. Transp. Harvest. Sea Resour.*, vol. 1, pp. 645-654, 2016.
- 20. ANSYS, ANSYS LS-DYNA User's Guide, Pennsylvania: Ansys, Inc., 2020.
- 21. S. Zhang, *The Mechanics of Ship Collisions*, Lyngby: Technical University of Denmark, 1999.
- 22. P. T. Pedersen and S. Zhang, "Absorbed energy in ship collisions and grounding-revising Minorsky's empirical method," *J. Ship Res.*, vol. 44, no. 2, pp. 140-154, 2000.
- 23. A. R. Prabowo, T. Tuswan, A. Nurcholis, and A. A. Pratama, "Structural Resistance of Simplified Side Hull Models Accounting for Stiffener Design and Loading Type," *Math. Probl. Eng.*, vol. 2021, no. 1, article no. 6229498, 2021.
- 24. R. Ridwan, S. Sudarno, H. Nubli, A. Chasan, I. Istanto, and P. S. Pratama, "Numerical Analysis of Openings in Stiffeners under Impact Loading: Investigating Structural Response and Failure Behavior," *Mekanika Majalah Ilmiah Mekanika*., vol. 22, no. 2, pp. 115-125, 2023.
- 25. S. Ehlers, "A procedure to optimize ship side structures for crashworthiness," *Proc. Inst. Mech. Eng. Part M J. Eng. Marit. Environ.*, vol. 224, no. 1, pp. 1-11, 2010.
- 26. A. R. Prabowo, A. Bahatmaka, and J. M. Sohn, "Crashworthiness characteristic of longitudinal deck structures against identified accidental action in marine environment: a study case of ship-bow collision," *J. Brazilian Soc. Mech. Sci. Eng.*, vol. 42, no. 3, article no. 584, 2020.
- 27. A. R. Prabowo, R. Ridwan, T. Tuswan, D. F. Smaradhana, B. Cao, and S. J. Baek, "Crushing resistance on the metal-based plate under impact loading: A systematic study on the indenter radius influence in grounding accident," *Appl. Eng. Sci.*, vol. 18, article no. 100177, 2024
- 28. F. Liu, R. Li, N. Su, and G. Feng, "Experimental and numerical investigations on EH36 steel plates subjected to quasi-static penetration and repeated dynamic impact loads," *Int. J. Impact Eng.*, vol. 198, article no. 105212, 2025.
- 29. M. S. Akbar, A. R. Prabowo, D. D. P. Tjahjana, F. B. Laksono, and S. J. Baek, "Assessment of designed midship section structures subjected to the hydrostatic and hydrodynamic loads: A convergence study," *Procedia Struct. Integr.*, vol. 33, pp. 67-74, 2021.
- 30. Z. Xiong, M. Ma, Y. Guo, and R. Li, "Study of energy absorption characteristics of coastal ship side structures based on collision accidents," *Ocean Eng.*, vol. 307, article no. 118079, 2024.
- 31. J. Pan, T. Wang, W. Z. Zhang, S. W. Huang, and M. C. Xu, "Study on the assessment of axial crushing force of bulbous bow for bridge against ship collision," *Ocean Eng.*, vol. 255, article no. 111411, 2022.
- 32. A. AbuBakar and R. S. Dow, "The impact analysis characteristics of a ship's bow during collisions," *Eng. Fail. Anal.*, vol. 100, pp. 492-511, 2019.
- 33. A. R. Prabowo, B. I. R. Harsritanto, D. M. Bae, J. M. Sohn, A. Bahatmaka, S. Samuel, and B. I. R. Harsritanto, "Progressive structural failure of the RoRo side hull during accidental powered-bow collisions," in the 6th International Conference on Science & Engineering in Mathematics, Chemistry and Physics, Jakarta, Indonesia, 2018.
- 34. B. Q. Chen, B. Liu, and C. G. Soares, "Experimental and numerical investigation on a double hull structure subject to collision," *Ocean Eng.*, vol. 256, article no. 111437, 2022.
- 35. E. S. Yeshanew, G. M. S. Ahmed, D. K. Sinha, I. A. Badruddin, S. Kamangar, I. M. Alarifi, and H. M. Hadidi, "Experimental investigation and crashworthiness analysis of 3D printed carbon PA automobile bumper to improve energy absorption by using LS-DYNA," *Adv. Mech. Eng.*, vol. 15, no. 6, 2023.
- 36. D. Hambissa, R. B. Nallamothu, and T. Andarge, "Analysis of Three-Wheeler Vehicle Structure at the Event of Side Pole Crash," *J. Eng.*, vol. 2022, no. 1, article no. 5490585, 2022.

- 37. H. Liu, K. Liu, X. Wang, Z. Gao, J. Wang, "On the Resistance of Cruciform Structures during Ship Collision and Grounding," *J. Mar. Sci. Eng.*, vol. 11, no. 2, article no. 459, 2023.
- 38. Z. Wang, K. Liu, G. Chen, and Z. Hu, "An analytical method to assess the structural responses of ship side structures by raked bow under oblique collision scenarios," *Proc. Inst. Mech. Eng. Part M J. Eng. Marit. Environ.*, vol. 235, no. 3, pp. 773-791, 2021.
- 39. I. M. Suci, G. Sitepu, M. Zubair, and M. Alie, "Longitudinal Strength Analysis Considering the Cargo Load on Very Large Crude Carrier (VLCC)," *Kapal Jurnal Ilmu Pengetahuan dan Teknolologi Kelautan*, vol. 18, no. 3, pp. 171-177, 2021.
- 40. D. Rosato and D. Rosato, Plastics Engineered Product Design, Amsterdam: Elsevier, 2003
- 41. A. I. Wulandari, R. J. Ikhwani, S. suardi suardi, R. S. Yani, A. N. Himaya, and A. Alamsyah, "Collision Analysis of a Self Propelled Oil Barge (SPOB) Using Finite Element Method," *Kapal Jurnal Ilmu Pengetahuan dan Teknologi Kelautan*, vol. 19, no. 2, pp. 101-111, 2022.